Relationship between Phenolic Adhesive Chemistry, Cure and Joint Performance. Part I. Effects of Base Resin Constitution and Hardener on Fracture Energy and Thermal Effects During Cure

Robert O. Ebewele[a]; Bryan H. River[b]; James A. Koutsky[c]

[a] Department of Chemical Engineering, Ahmadu Bello University, Sunaru-Zaria, Nigeria [b] Forest Products Laboratory, Forest Service, U. S. Department of Agriculture, Madison, Wl, U.S.A. [c] Department of Chemical Engineering, University of Wisconsin, Madison, Wl, U.S.A.

PLEASE SCROLL DOWN FOR ARTICLE

Relationship between Phenolic Adhesive Chemistry, Cure and Joint Performance.

Part I. Effects of Base Resin Constitution and Hardener on Fracture Energy and Thermal Effects During Cure†

ROBERT O. EBEWELE

Department of Chemical Engineering, Ahmadu Bello University, Sunaru-Zaria, Nigeria

BRYAN H. RIVER

Forest Products Laboratory, Forest Service, U.S. Department of Agriculture, Madison, WI 53705, U.S.A.

and

JAMES A. KOUTSKY‡

Department of Chemical Engineering, University of Wisconsin, Madison, WI 53706, U.S.A.

In this study the relationships between the composition of phenol resorcinol-formaldehyde resins and paraformaldehyde concentration in the adhesive were explored, using DSC, IR, GPC, and solubility measurements. Differences of chemical composition between base resins and adhesives were compared to the fracture toughness of adhesive bonds.

The cure temperature and cure time effects upon fracture toughness were also investigated. Fracture toughness tests were performed with bonded hard maple tapered double-cantilever beam cleavage specimens.

---

† Work done at University of Wisconsin.
‡ To whom inquiries should be addressed.

The fracture toughness of most adhesive systems increased with increasing paraformaldehyde concentrations to a level of 10 to 15 parts per 100 parts of resin. The fracture toughness initially increased, maximized, and then decreased with cure time. Higher cure temperatures accelerated the process. Higher resorcinol content gave higher fracture toughness values, and larger thermal responses by adhesives in DSC measurements correlated with greater fracture toughness.

Some tentative relationships between cure and fracture toughness are examined. Implications for improving the usefulness of accelerated-aging studies are discussed.

INTRODUCTION

The durability or permanence of a bonded joint in service is an important consideration in the acceptance of an adhesive for a particular end use. Ideally, the most reliable information on durability characteristics of a given adhesive or adherend-adhesive system should be developed over a period of years in which the test samples are subjected to conditions comparable to those of the glued product in service. However, such long-term tests are impractical. Therefore, greater reliance must be placed on results obtained from short-term accelerated tests. To date, however, no entirely satisfactory correlation has been found between accelerated test data and actual long-term service results. Thus, an unresolved discrepancy exists between accelerated test results and real-time service performance of adhesive joints.

A plausible approach to bridging this gap between accelerated test data and real-time results is a fundamental understanding not only of the properties of the elements constituting an adhesive joint but also their contribution, both separately and jointly, to the overall integrity of the bonded assembly. Wood-phenolic adhesive joints constitute the subject of our investigations. In previous papers[1,2] we reported the effects of the intrinsic nature of wood (wood anisotropy) and wood processing (surface roughness) on adhesive joint-fracture energy. In the first part of this paper, we will discuss the effect of base resin constitution on joint performance while in the second part we will report the thermal effects on adhesive joint performance.

The cure of phenolic resins has received extensive investigation by three principal groups led by Zinke,[3] von Euler[4] and Hultzch.[5] These groups found that the process of phenolic-resin cure occurs in two stages:

1) Formation of ether-linked polymers by condensation between two adjacent methylol groups with loss of water.

2) Breakdown of these ether-linked polymers by loss of formaldehyde at longer periods of cure or higher cure temperatures (170°C). While there is general agreement among the three groups that ether linkages are first formed, there is disagreement as to what happens during the second stage of breakdown of the ether linkages. The Zinke group argues that the ether bridges partly split to give methylene bridges and also partly decompose to

give phenolic aldehydes and methylated phenols. The von Euler and Hultzch groups, on the other hand, postulate quinone methide formation.

Lilley[6] considered the first stage of the cure process to be an ionic reaction while the solvent was present, while the second stage in the solid phase was supposedly a free radical process. In both sequences, the primary reaction was considered to be the formation of methylene bridges while the ether-forming reaction was of minor consequence. Conley and Bieron,[7] and Jackson and Conley,[8] agreed with Lilley's conclusion that ether linkages are absent in cured phenolic resins. They proposed a primary oxidation route for phenolic resins in which the diphenyl-methane unit is converted to benzophenone linkages.

Yamao et al.[9,10] have also studied both acid hardening and heat curing of resole-type phenolic resins using infrared spectroscopy. They reported that the formation of the dimethylene ether linkage, due to reactions between methylol groups, was the initial major reaction. The subsequent decomposition of these ether linkages coincided with a rapid increase in the carbonyl group of quinone and quinone methide. The extent and rate of decomposition of the ether linkage depended on the formaldehyde/phenol (F/P) mole ratio and the reaction temperature. For the base-catalyzed reactions, carbonyl formation was minimal at low temperatures (120°C). However, for the acid-catalyzed reactions, a small amount of carbonyl group was detected even at 60°C. This was attributed to the oxidation of the methylene linkage formed by the reaction of methylol group with active p-position as opposed to dimethylene ether decomposition.

All of the literature cited above was concerned with cure and possible degradation mechanisms of phenolic resins. In this paper we will attempt *via* fracture mechanics and chemical analysis to find correlations of adhesive chemistry and joint strengths.

EXPERIMENTAL

As in previous work,[1,2] the principles of fracture mechanics were used to measure the fracture toughness of adhesive bonds while differential scanning calorimetry (DSC), infrared spectroscopy (IR), gel permeation chromatography (GPC), and solubility measurements were used to evaluate the adhesive chemistry. The preparation of the adherends, bonding procedures, and fracture tests were as described in previous papers.[1,2]

The adhesives used were based on a commercial phenol-resorcinol resin (Koppers' Penacolite G4411) and a laboratory-synthesized resin. The recipe for the laboratory resin is given in Table I. The fillers were walnut shell flour and mica, and the hardener was paraformaldehyde from Celanese Corporation. The adhesive formulation was 100 parts of resin to 10 parts of

TABLE I

Recipe for laboratory synthesized resin (from Weyerhaeuser Co.)

Ingredients			
90% Phenol[1]	27.35	Resorcinol	28.82
91% Paraflake[1]	9.51	2nd Water	31.44
Calcium acetate	0.26		
1st water	2.62		100.00

Procedure

1. Charge the kettle with phenol, paraflake, calcium acetate, and 1st water.
2. Adjust the temperature to 30°C and heat to reflux in 75 min using a steady rate of heating. Cooling water may be needed to hold the slight exotherm at 80°C. Reflux temperature 107°C.
3. Reflux for 105 min. The temperature will decrease during this period.
4. Cool the resin just enough to stop boiling and add the resorcinol. Heat the resin to reflux and reflux for 15 min.
5. Add 2nd water and heat to reflux.
6. Reflux to viscosity of "F" on the Gardner-Holdt Scale.
7. Cool to 25°C.
8. Adjust pH to 8.5 to 9.0 with 50% NaOH.

[1] Adjust for assay and make corresponding adjustments in 1st water.

filler to 5 to 25 parts of paraformaldehyde. Cure conditions were 85°C for 1 h for the studies involving effects of base resin constitution while the thermal effects were explored using the Koppers' resin with only 10 phr paraformaldehyde with 50, 85, 100, 120 and 150°C cure temperatures and cure time varying 1 to 20 h.

Adherends

Hard maple (*Acer saccharum* Marsh) was chosen as the wood substrate because of its high modulus and controllable glue assimilation. Rough lumber for the specimens was conditioned to equilibrium at 23°C and 44% relative humidity (RH) ($=8\%$ EMC). After conditioning, the specimens were cut into tapered beams having a constant grain angle, 20°, to the bonding surface and tapered to the appropriate shape which was established in previous work.[1,2] The taper of the beams was chosen as 52.36 m^{-1} for all specimens tested.[2] This taper was found to be optimum for bonding and fracture tests.

Differential scanning calorimetry (DSC)

The DSC was employed for screening adhesive formulation variables and deriving preliminary bonding process conditions. Five grams of the resin and

the appropriate amount and type of filler and the curing agent were mixed thoroughly in a beaker for 5 minutes. From this, between 5 and 10 mg was weighed very accurately in a DuPont aluminum-coated pan and then sealed hermetically. Thermograms were then obtained on a DuPont 900 DSC unit using a similarly sealed empty pan as the reference. A heating rate of 10°C/min and a range setting of 4 mcal/sec were employed. The temperature range of the scans was 20–300°C. The instrument was calibrated by measuring the heat of fusion of indium. Areas under the peaks were measured with a planimeter with measurement errors of less than 10%.

Infrared studies

During bonding, a portion of each adhesive formulation (usually 30 g) was transferred to a metal can and then cured under the same conditions (in the same oven for the same cure time) as the adhesive joint. Soon after removal from the oven, the adhesive was placed in a thick, tightly sealed (ziplock) polyethylene bag and stored in a sub-zero degree room until infrared measurements were made. For the infrared measurements, a small portion of the cured adhesive was ground to a fine powder, mixed with potassium bromide (KBr) powder (1.5 parts resin/300 parts KBr, weight basis) and pressed into a pellet. Infrared absorption scans were carried out on a Beckman 12 infrared spectrophotometer.

Gel permeaton chromatography (GPC) and solubility measurements

For these measurements, the remaining portion of the cured adhesive was ground to 20 mesh. Ten grams of the ground adhesive were weighed into an extraction thimble. This was placed in a specimen bottle containing 100 ml of tetrahydrofuran (THF). This amount of THF was sufficient to cover the adhesive completely. The bottle was sealed tightly and left at room temperature (c. 24°C) for 5 to 6 weeks. At the end of this period, a portion of the solution was filtered and 6–10 ml of the filtered solution was injected into the chromatograph (Walters Model 501) which contained five styragel columns in series. THF was used as the solvent. A range of molecular weights of $< 10^4$ to 10^8 could be measured. After the GPC measurement, the thimble was then removed and dried in an oven at 70–72°C to a constant weight. A chromatogram of the uncured resin was also obtained by injecting a 1% THF solution into the chromatograph.

Bonding

The adhesive was mixed vigorously by hand for 10 minutes and then handbrushed on both surfaces of the beams to be mated as uniformly as possible. Open assembly time was less than 30 seconds. A small Mylar or Teflon film of 2.54×10^{-3} cm (1 mil) thickness was inserted at the jaw of the specimen to provide the initial flaw. The specimens were placed in a press capable of holding two specimens, as shown in Figure 4 of Ref. 2. The closed assembly time was 30 minutes. Glueline pressure, 1.03–1.17 MPa (150–170 psi), was measured by a precalibrated compressometer. Before curing, excess glue was cleaned off the joint with a knife. The press with the samples was placed in a forced-air oven maintained at 85°C (± 1°C) and cured for 1 h. Generally the applied glueline pressure dropped considerably by the time the specimens were removed from the oven, due to the combined effects of wood drying and metal expansion.

Fracture testing

After bonding and conditioning at 25°C, 44% RH for 3 days, the samples were fractured using a Riehle Ametek testing machine at 0.2 mm/min crosshead speed. Sample deflections at the grips was monitored by a LVDT—Daytronic Signal Conditioner, Model 300D. Load and LVDT displacement was recorded. Details are given in Ref. 2.

RESULTS OF STUDIES ON BASE RESIN CONSTITUTION

Differential scanning calorimetry (DSC)

Figure 1 shows the thermograms for the commercial resin (Koppers' Penacolite G4411(A)) and the laboratory-synthesized phenol-resorcinol-formaldehyde (PRF) resin (B). The adhesive formulation in both cases was 100 parts resin to 10 parts paraformaldehyde and no fillers, i.e., 100/10/0. Observe that the exothermic peak maxima and the endothermic peak minima occur at approximately the same temperatures (c.85 and 215°C, respectively). For the laboratory resin the heat liberated at the exotherm during cure (ΔH_{exo}) was 47 cal/g, compared with 29 cal/g for the commercial resin. In contrast, while the heat absorbed at the endotherm (ΔH_{endo}) was 172 cal/g for the commercial resin, that for the laboratory-synthesized resin was 133 cal/g.

With increased addition of paraformaldehyde to the adhesive:

1) The temperature of the exothermic peak maximum decreased nearly linearly from 85 to 70°C for 10 phr, and 25 phr paraformaldehyde concentrations, respectively.
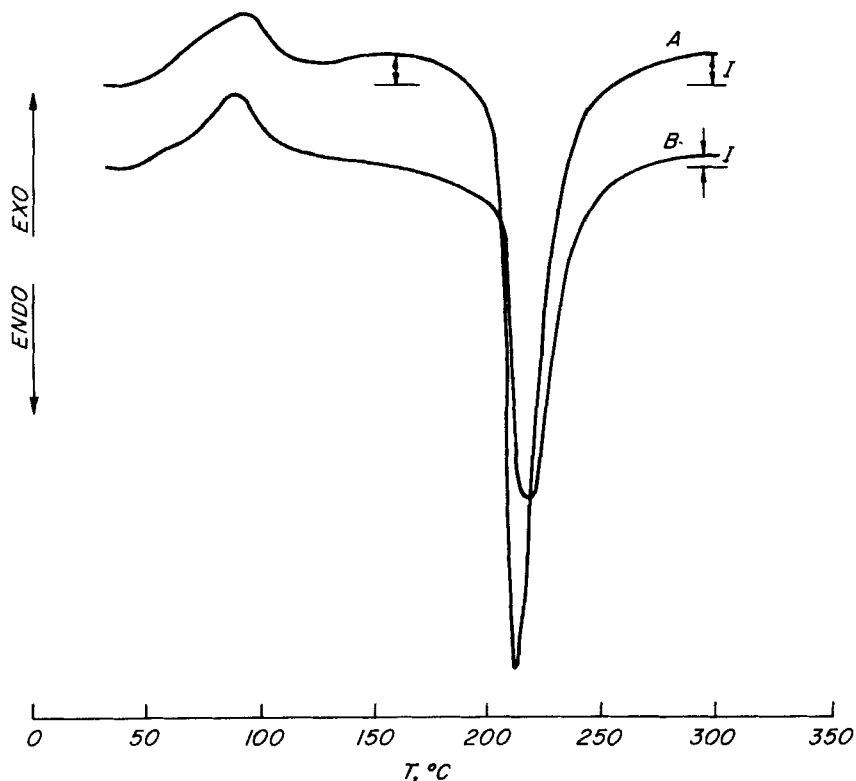
FIGURE 1   Relative thermal characteristics of the commercial (G4411) resin (A) and the laboratory resin (B). Observe the differences in the baseline shift (I) (exothermic direction) in both resins. For the commercial resin, ΔH_{exo} and ΔH_{endo} were 29 cal/g and 172 cal/g, respectively. The corresponding values for the laboratory resins were 47 cal/g and 133 cal/g.

2) The heat of reaction at the exotherm (ΔH_{exo}) showed a maximum at about 10 phr.

3) The heat of reaction at the endotherm (ΔH_{endo}) increased from approximately 180 cal/g at 5 phr to 220 cal/g at 20 phr, and remained nearly level for greater amounts of paraformaldehyde.

Infrared measurements

Infrared absorption characteristics of the parent (uncured) laboratory and commercial resins and their unfilled adhesive formulations with para-formaldehyde showed some differences. The change in the infrared absorption behavior, with an increase in paraformaldehyde concentration for both

adhesives, is shown in Figure 2 and tabulated in Table II. Different researchers assigned different absorption bands to the same chemical group. This is probably due to slight structural differences between the phenolic resins studied by the individual researchers. In view of the possibility of such shifts in the absorption bands for a particular chemical group, the methylol OH group appears to be represented by the 1045 cm^{-1} in the commercial resin but by the 1000 cm^{-1} in the laboratory resin.

Chow[11] has reported that PRF resins with resorcinol contents greater than 5% exhibit two strong bands: 960 and 1140 cm^{-1}. He attributed the presence of these bands to resorcinol, noting that they were assigned to inplane bending modes of hydrogen atoms in 1,3 substituted benzene ring by Nakanishi.[12] In

TABLE II

Relative infra-red absorption characteristics of two PRF resins

Adhesive formulation	Absorption band cm^{-1}	Commercial resin G4411	Laboratory-synthesized resin
100/0/0 (Pure resin)	1510–1450	Sharp	Slightly unresolved
	1220	Broad	Narrow
	1300, 1100	Small absorption	Small absorption but relatively greater than G4411
	1045	Sharp and relatively intense	Virtually absent
	Other bands	Essentially the same for the two resins (qualitatively)	
100/10/0 cured at 85°C for 1 h	1390, 1305 1153, 1075 976, 965, 814	Disappeared	Disappeared
	1100	Enhanced relative to pure resin	Relative enhancement much greater than G4411
	1000	Absent	Present
Varied from 100/5/0 to 100/25/0 cured at 85°C for 1 h	1100	Increased slightly to a constant level	Increased and then decreased; increase much greater than G4411 (Figure 3)
	760	Decreased to a constant level	Increased and then decreased; increase much greater than G4411 (Figure 3)
	1045	Decreased to a constant level	Absent
	1000	Absent	Fairly low initially, then jumped to constant level
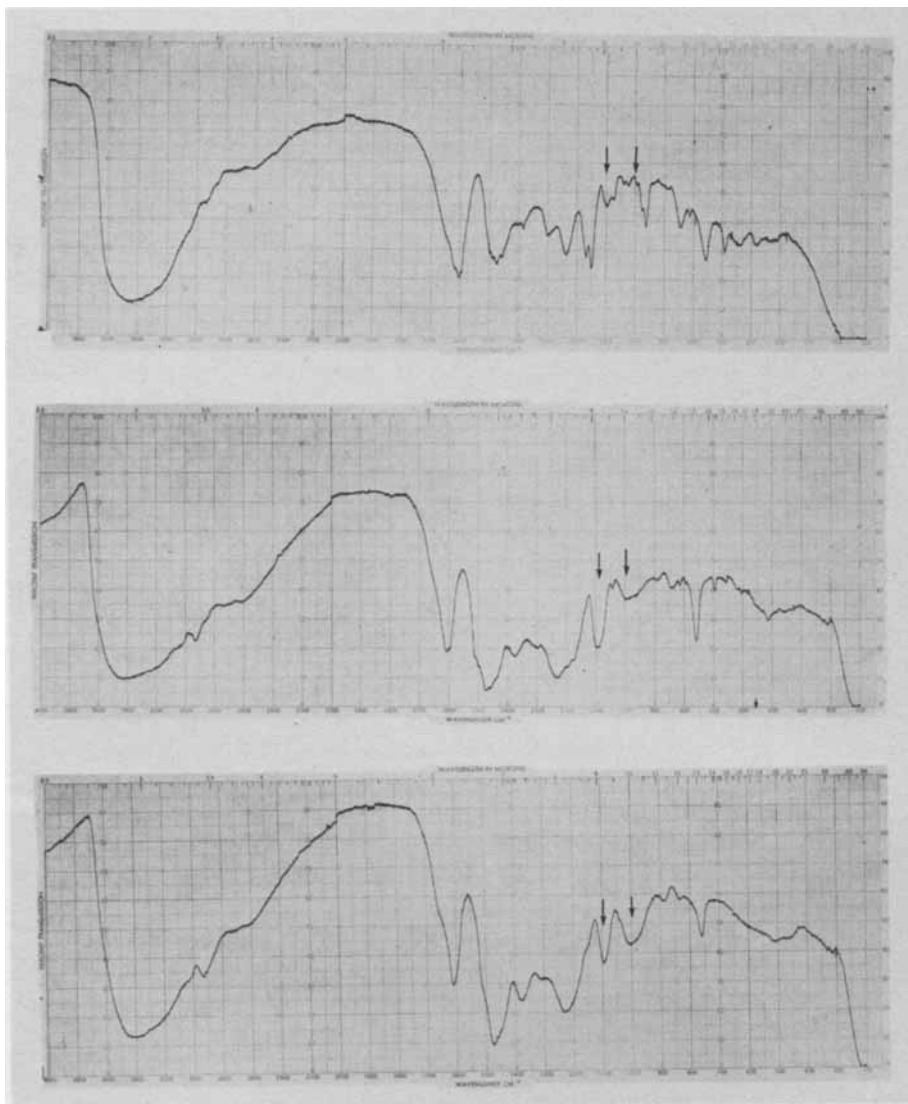
FIGURE 2 Infrared absorption of the laboratory resin adhesive as a function of para-formaldehyde concentration: A = pure (parent) resin; B = adhesive formulation 100/10/0; C = adhesive formulation 100/20/0 cured at 85°C for 1 h. Note the increase in 1000 cm^{-1} band and the decrease in 1100 cm^{-1} band.

a subsequent paper, Chow[13] used one of the bands assigned to resorcinol (1140 cm^{-1}) to derive an empirical relationship for determining the resorcinol content of PRF resins. He showed that the absorbance ratio A_{1140}/A_{1220} was related to the resorcinol content of PRF resins by the equation:

$$X = 29.41\ Y - 10.41$$

$$5 \leqslant X \leqslant 50$$

where:

   X = percentage resorcinol content (based on added solids)
   Y = absorbance ratio: A_{1140}/A_{1220}

By this relationship we estimated the resorcinol content of the laboratory resin to be about 48%. This compares well with the actual value of 46% from the recipe (Table I). The resorcinol content for the commercial resin was estimated to be 18%. (The actual value was not given by the suppliers.) Recall that from the DSC results, the heat evolved at the reaction exotherm (ΔH_{exo}) was 47 cal/g and 29 cal/g for the laboratory and the commercial (G4411) resins, respectively (adhesive formulation 100/10/0). Although the heat evolved at the reaction exotherm, ΔH_{exo}, is not exactly proportional to the amount of resorcinol in both resins, the relative value of ΔH_{exo} for both resins indicates that the exothermic reaction is strongly due to the resorcinol content of the PRF resin adhesive.

With an increase in the added paraformaldehyde, the two resins behaved rather differently. Figures 3 and 4 show the trends in the absorption characteristics of three bands relative to the same absorption bands in the pure resin. The 1610 cm^{-1} was used as the internal standard (Yamao, et al.[9]). The dimethylene ether linkage in the commercial G4411 resin adhesive increased slightly to a constant level (relative to the pure parent resin); the laboratory resin adhesive, on the other hand, gave a much greater dimethylene ether content which increased initially and then dropped precipitously as cure proceeded. The methylol OH in the laboratory resin was virtually nonexistent initially but they grew to a constant high level. In contrast, the methylol OH group decreased modestly to a constant level in the commercial resin. The aromatic ring substitution pattern as reflected by the relative absorption trend of the 760 cm^{-1} band showed that while there was little ring substitution change in the commercial resin, ring substitution increased with increased addition of paraformaldehyde in the laboratory resin.

Gel permeation chromatography and solubility measurements

Figure 5 shows the change in the soluble fraction of the adhesives with increased addition of paraformaldehyde for the commercial and the lab-
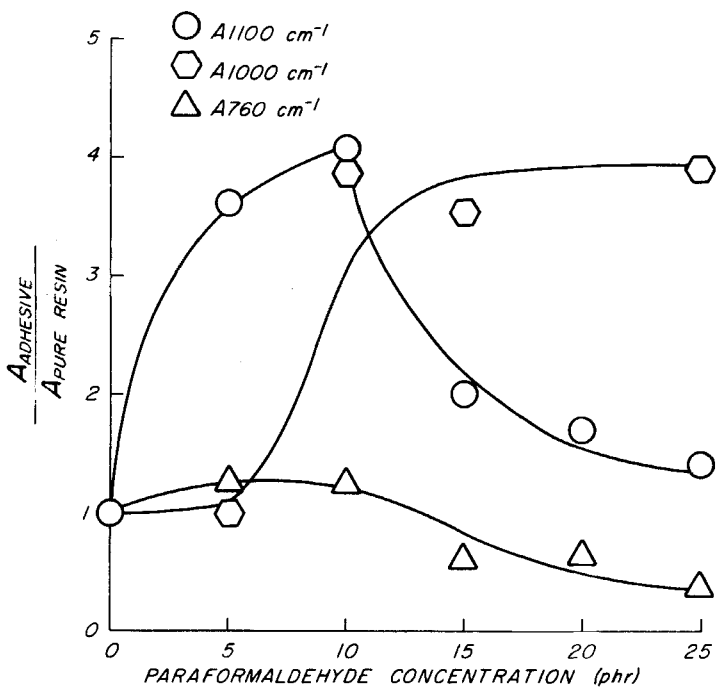
FIGURE 3   The amount of ether linkage (1100 cm^{-1}) methylol OH (1000 cm^{-1}) and extent of crosslinking (760 cm^{-1}) in the laboratory adhesive relative to the laboratory resin as a function of paraformaldehyde concentration.

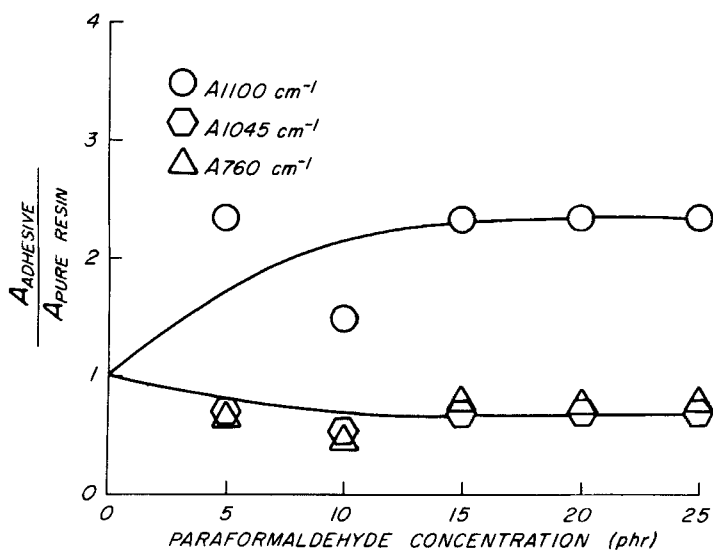FIGURE 4   The amount of ether linkage (1100 cm^{-1}), methylol OH (1045 cm^{-1}) and extent of crosslinking (760 cm^{-1}) in the commercial adhesive relative to the commercial resin as a function of paraformaldehyde concentration.

oratory resins, respectively. In both cases, three distinct molecular species (I, II, and III) are present in the soluble fraction of the adhesives as well as in the parent resin. Observe that the peaks for the three species in the parent laboratory resin (dotted line in Figure 5b) occur at relatively lower retention volumes than the corresponding peaks for the corresponding species in the
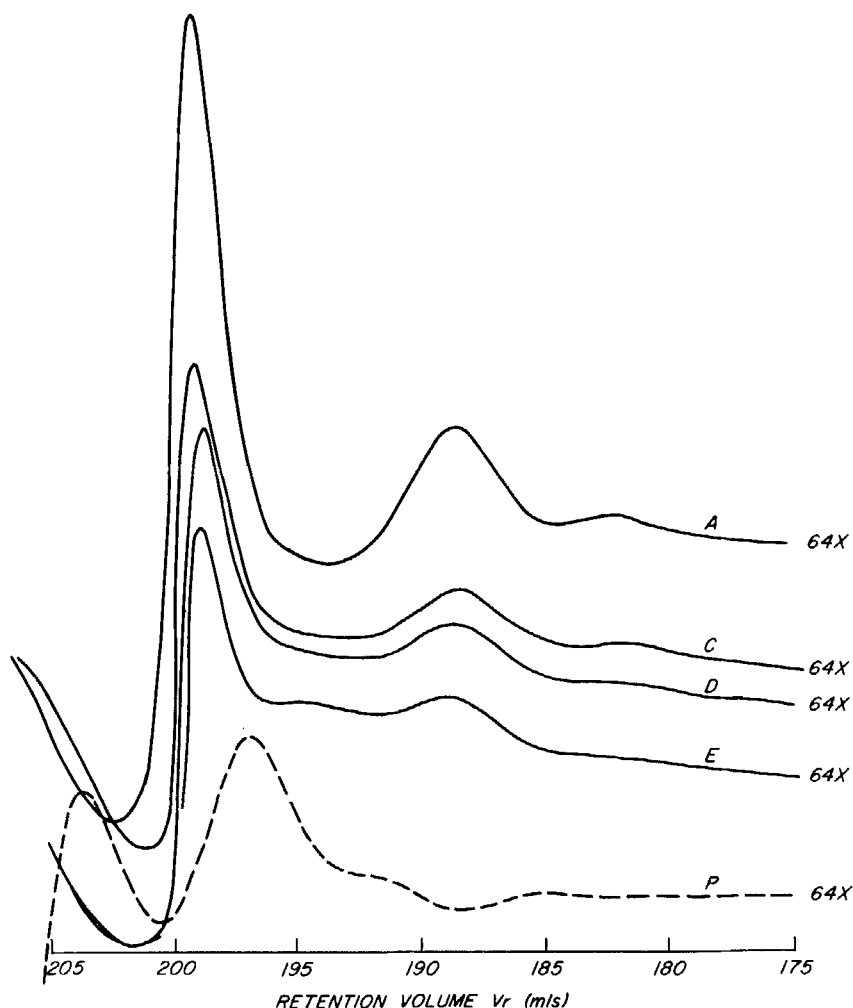
FIGURE 5a   The gel permeation chromatogram of commercial resin adhesive (A to E) in relation to paraformaldehyde concentration. (A = 5, C = 15, D = 20, E = 25 phr, P = pure resin cured 1 h at 85°C. Ordinate scale in arbitrary units of concentration.
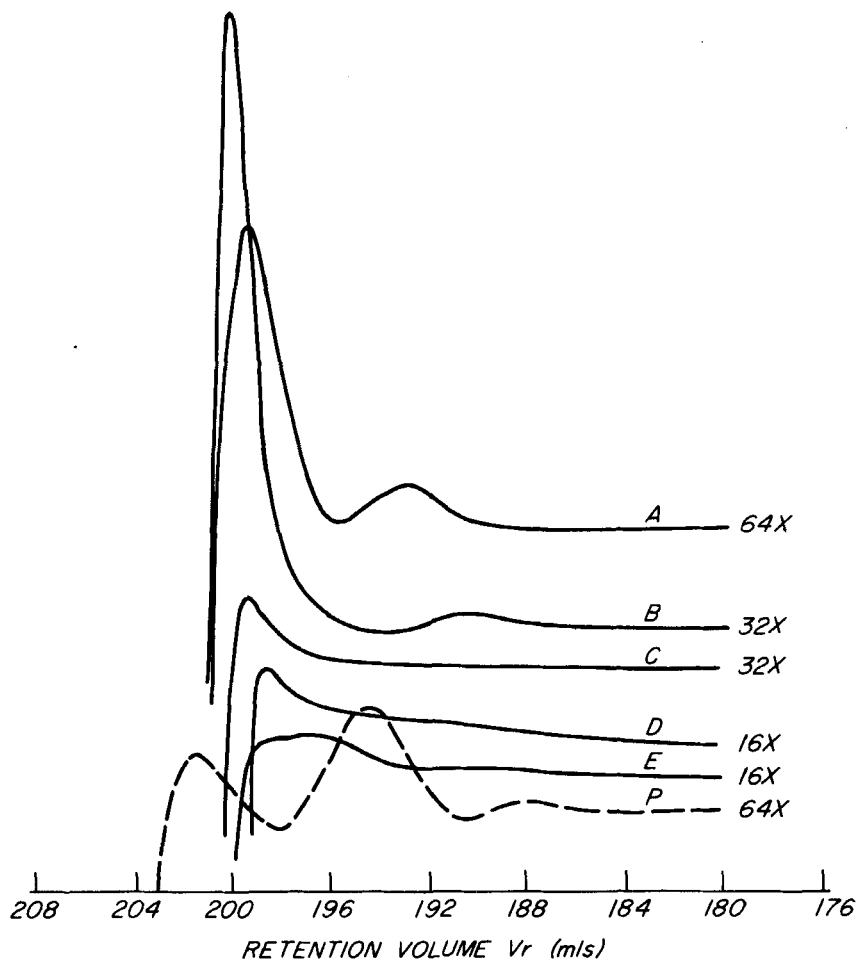
FIGURE 5b The gel permeation chromatogram of the laboratory resin adhesive (A to E) in relation to paraformaldehyde concentration (A = 5, B = 10, C = 20, E = 25 phr, P = pure resin curved 1 h at 85°C). (Note attenuation scale change of curves B, C, D and E when comparing 5a to 5b—16 × data is twice the sensitivity of 32 × and four times 64 × data.)

parent commercial resin (dotted line, Figure 5a). The elution volumes of the species in the soluble fraction of the adhesive are lower than those of corresponding species in the parent resin. During cure, species II appears to be consumed at a faster rate relative to species III in both resins. A remarkable difference in reactivities, however, exist between both resins. Only a slight decrease occurs in the amount of the different species as the paraformaldehyde

added to the commercial resin is increased (Figure 5a). In contrast, for the laboratory-synthesized resin adhesives, the addition of $\geqslant 5$ phr paraformaldehyde obliterates species I; and at additions $\geqslant 15$ phr, species II is drastically reduced (Figure 5b). (Note that the sensitivity of the instrument at $64 \times$ attenuation had to be doubled, $32 \times$, and quadrupled, $16 \times$, for the peaks to be observable at higher paraformaldehyde additions to the laboratory resin.)

Figure 6 shows the change in the soluble fraction of adhesive cured at 85°C for 1 h with increased paraformaldehyde addition. The soluble fractions at 5 phr added paraformaldehyde were the same for both the laboratory resin adhesive and the filled and unfilled commercial resin adhesives within the limits of experimental error. The soluble fraction of the commercial resin adhesives modestly increased in a linear fashion with increasing amounts of added paraformaldehyde. In contrast, the soluble fraction for the laboratory
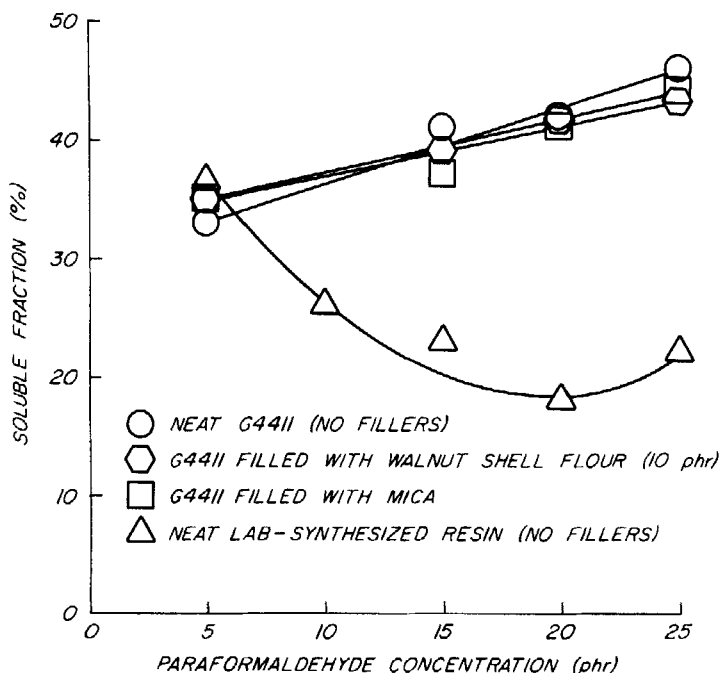

FIGURE 6   The soluble fraction of the commercial (G4411) resin and the laboratory resin adhesive as a function of paraformaldehyde concentration. Note soluble fraction increased in the commercial resin adhesive while it decreased in laboratory resin adhesive up to 25 phr added paraformaldehyde. The filled and unfilled commercial resin adhesive had identical soluble fractions.

resin adhesive decreased to a somewhat constant value with increasing paraformaldehyde concentration. However, there was a slight increase in the soluble fraction of the laboratory resin at 25 phr added paraformaldehyde.

Fracture energy

Figure 7 compares the fracture initiation energies for joints from both filled (mica and walnut shell flour) and unfilled commercial resin adhesives. The fracture initiation energies of the corresponding joints from the laboratory resin adhesive cured at 85°C for 1 h are shown in Figure 8.

For joints derived from the neat commercial resin adhesive, the fracture energies (G_{1c} and G_{1a}) increased continuously with increasing paraformaldehyde. In contrast, joints derived from the filled commercial adhesives increased initially and then decreased at paraformaldehyde concentrations greater than 10 phr (Figure 7). From Figure 7 it can be seen that over the entire range of added paraformaldehyde, joints from the mica-filled adhesive had the

FIGURE 7   Comparison of the fracture initiation energies as a function of paraformaldehyde concentration for specimens bonded with filled and unfilled commercial resin adhesive. Note that the energy for specimens from filled adhesive showed a maximum in contrast to the continuous increase for specimens derived from the unfilled adhesive.
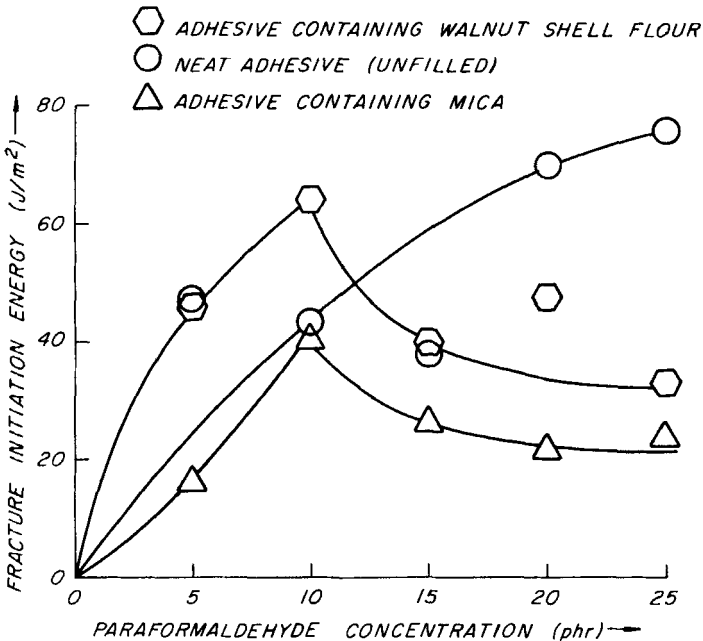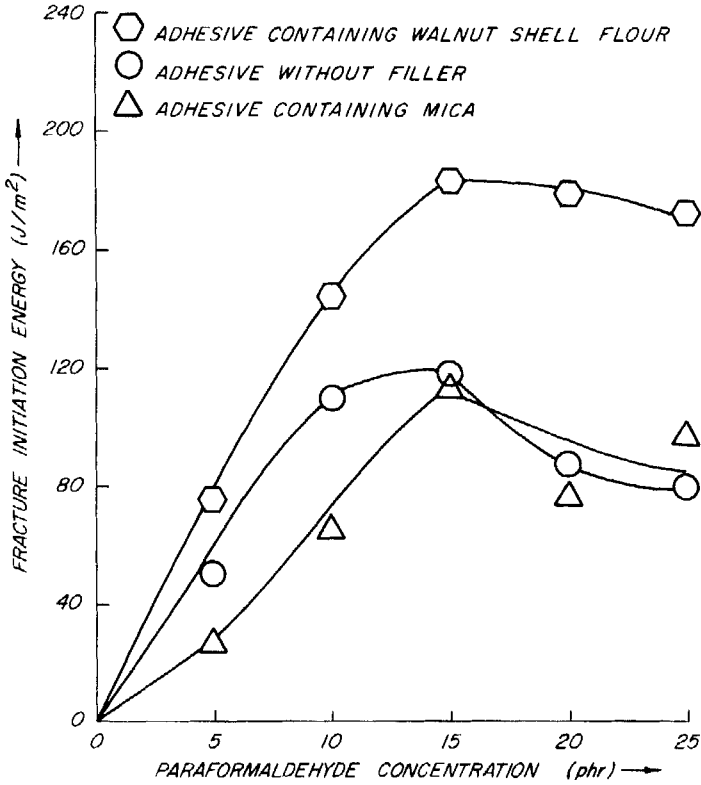
FIGURE 8   Comparison for the fracture initiation energies of a function of paraformaldehyde concentration for specimens bonded with filled and unfilled laboratory-synthesized resin adhesive. Note the relative magnitude of fracture energies.

lowest fracture energy. Joints from the walnut shell flour-filled adhesive generally had the highest fracture energy except at high paraformaldehyde concentration. It is possible that at these high paraformaldehyde concentrations that longer, more flexible, methylene ether links are formed in the unfilled resin acting as a "plasticizer" and giving greater toughness for this system.

For the joints bonded with the filled and unfilled laboratory resin adhesive, the fracture energies increased initially and then decreased with additional paraformaldehyde. The load-deflection recordings for the joints of mica-filled laboratory resin adhesive showed stable crack propagation at 5 phr added paraformaldehyde. However, at added paraformaldehyde equal to or greater than 10 phr, unstable crack propagation occurred. This transition was unique.

Notice that up to and including 15 phr added paraformaldehyde, the joints from the mica-filled adhesives were less tough than neat resin adhesive joints; but beyond this point, their toughness was roughly equal (Figure 8). The joints from the walnut shell flour-filled adhesive had the best strength performance (Figure 8).

Comparing Figures 7 and 8, it can be seen that the joints made from the laboratory resin adhesive had higher fracture energies than the corresponding joints from the commercial resin adhesive.

RESULTS ON THE STUDIES OF THERMAL EFFECTS DURING CURE

Infrared studies

Figure 9 shows the representative trends of the infrared absorption bands, with the 1610 cm^{-1} band used as the internal standard. Only those spectra for the adhesives cured at 50 and 150°C are shown in these figures. Relative to the parent resin, the ether linkage (1100 cm^{-1}) first increased and then decreased with cure time. The severity of the decrease appeared to increase with increasing cure temperature. (Compare Figures 9a and 9b.) The methylol OH absorption band (1053 cm^{-1}) and the 760 and 820 cm^{-1} bands (not shown),
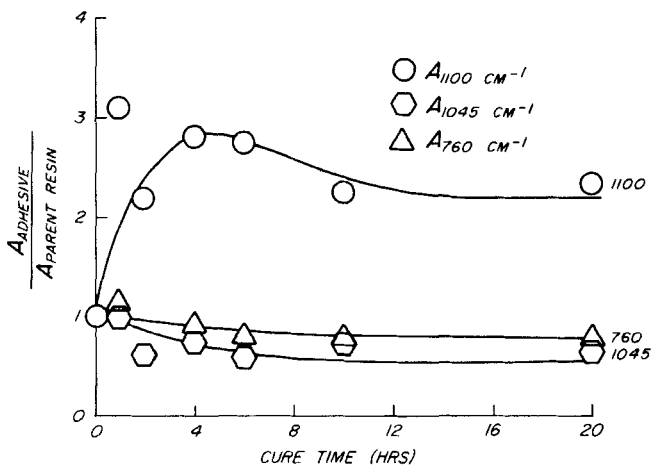

FIGURE 9a   Effect of cure time on the infrared absorption characteristics of an unfilled Penacolite G4411 resin with 10 phr paraformaldehyde. Cure temperature = 50°C.
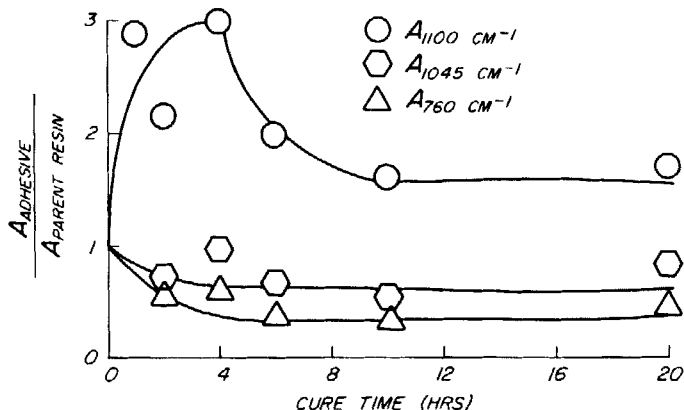
FIGURE 9b   Effect of cure time on the infrared absorption characteristics of unfilled Penacolite G4411 resin with 10 phr paraformaldehyde. Cure temperature = 150°C.

which are indicative of the degree of substitution on the benzene ring, decreased to a nearly constant value.

Figure 10 depicts the chromatogram for the adhesive cured for various lengths of time at 50°C. Similar trends were observed at the other cure temperatures. It is appearent that, with increasing cure time (at each cure temperature), no noticeable change in the relative elution volumes for the various species occurred. However, a sizeable decrease in the amount of all species is observed. This decrease is accentuated with increasing cure temperature.

Figure 11 shows the decrease in the soluble fraction of the cured adhesive with cure temperature. For the adhesives cured at 50, 85, and 100°C, the soluble fraction decreased continuously with increasing cure time. Note, however, that for the adhesives cured at 120 and 150°C, the soluble fraction decreased initially and then increased with a longer cure time. The minimum occurred at an earlier time for adhesives cured at 150°C than for those cured at 120°C.

Figure 12 shows the typical behavior of fracture initiation and arrest energies with cure time at an 85°C cure temperature. At each cure temperature, the fracture energies increased initially, passed through a maximum, and then decreased with increasing cure time. Figure 13 compares the fracture initiation energies at various cure temperatures. Notice that specimens cured at 85°C had the highest fracture energy over the entire cure period with the exception of one anomalous specimen at 150°C. At short cure times, the fracture energy rapidly increased for all cure temperatures with increasing cure time. At cure times greater than 10 h the fracture initiation energies appear nearly

independent of cure time. The maximum in the fracture energy-cure time profile occurred at 4 h for specimens cured at 85°C, decreased to 2 h for those cured at 100°C, and to about 1 h for specimens cured at 120 and 150°C. Specimens cured at 50°C seemed to depart from the above pattern of behavior. The fracture initiation energy in this case was lower than those of specimens
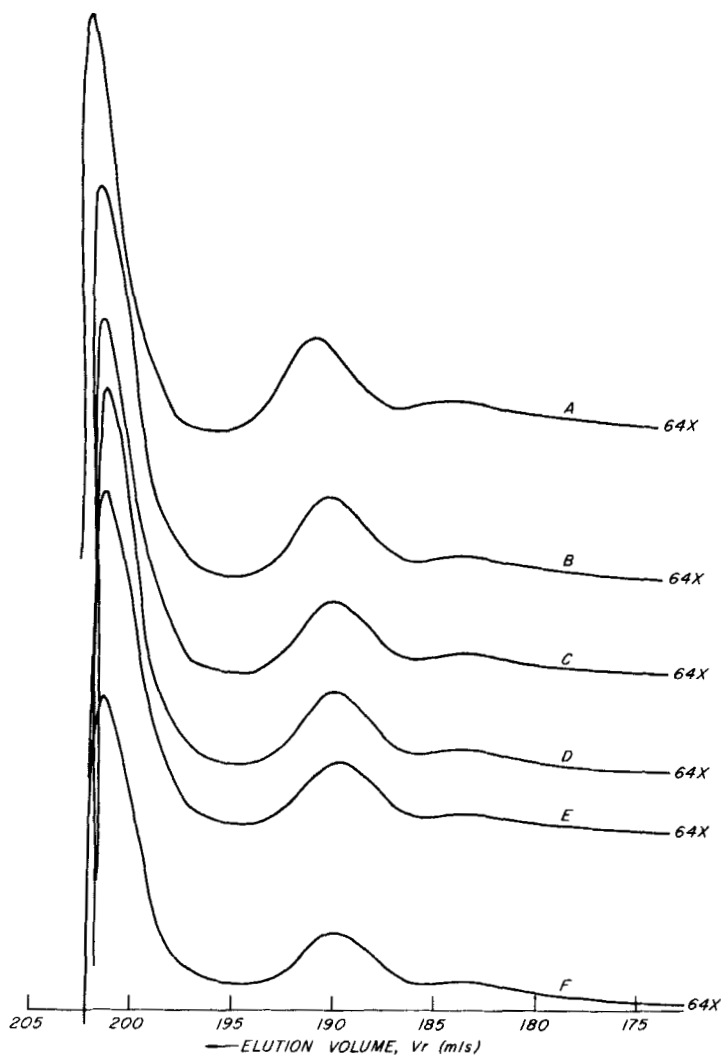

FIGURE 10 Change in the gel permeation chromatograms of the soluble fraction of adhesive (100/10/0) cured at 50°C for various lengths of time. (A = 1 h, B = 2 h, C = 4 h, D = 6 h, E = 10 h, F = 20 h) Note decrease in amount of species I, II, and III with increase in cure time.
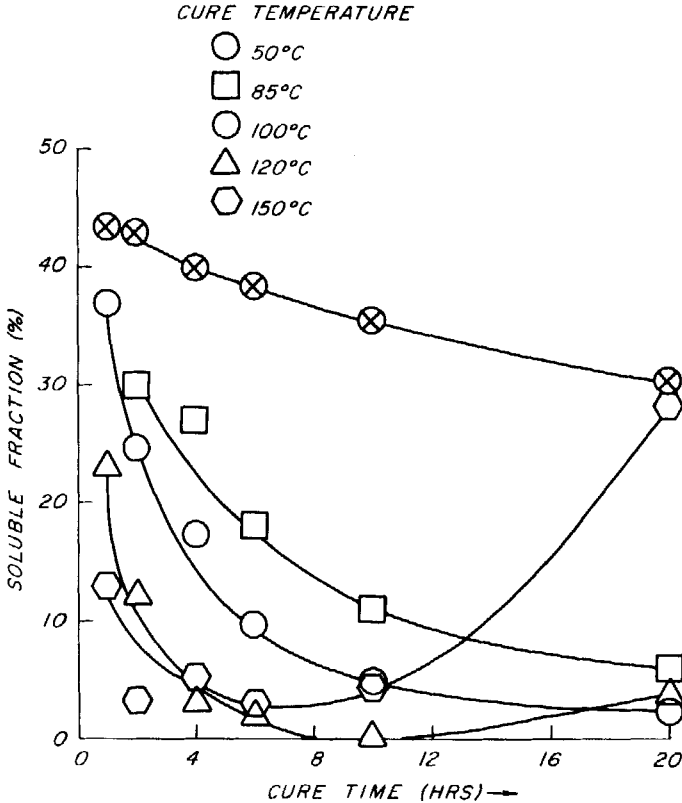
FIGURE 11   The soluble fraction of adhesives cured at different temperatures as a function of cure time. Note that while the soluble fractions for adhesives cured at 50°, 85°, and 100°C decreased with increasing cure time, those for adhesives cured at 120° and 150°C showed a minimum.

cured at 85 and 100°C, but higher than those of specimens cured at 120°C and 150°C. The maximum in the fracture energy-cure time profile occurred at about 3 h for specimens cured at 50°C.

DISCUSSION

Base resin constitution

The observed infrared absorption pattern for the various chemical groups appears related to the extent of reaction during resin synthesis and the ratio of phenol and/or resorcinol to formaldehyde in the parent resin. Quite possibly

FIGURE 12 Variation of fracture initiation and arrest energies with cure time for specimens cured at 85°C. (Adhesive formulation: 100/10/0.) I_A and I_B indicate $(G_{Ic} - G_{Ia})$ at two different states of cure but showing the same G_{Ic}.

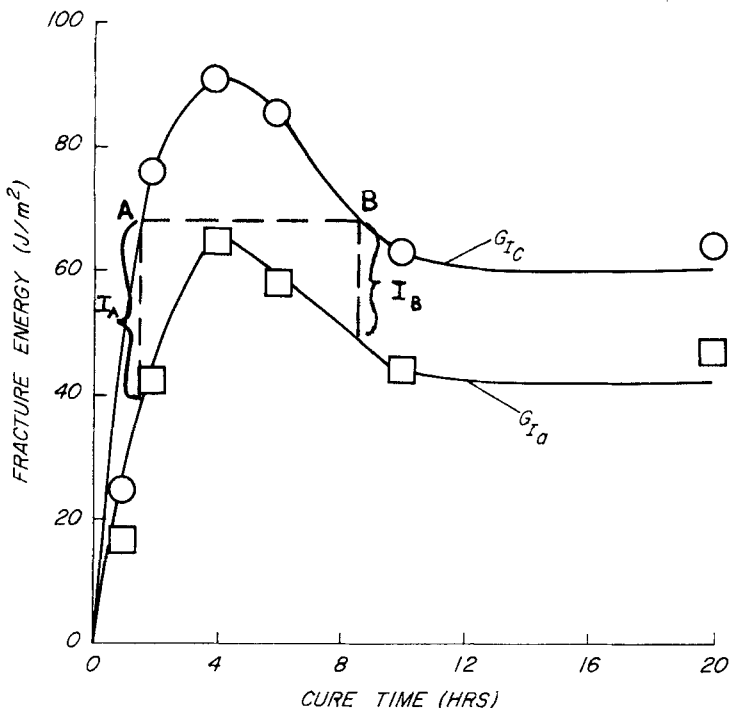the condensation of methylol groups to dimethylene ether linkages may have been more advanced in the laboratory-synthesized resin than in the commercial resin. With the 1610 cm^{-1} absorption band as the internal standard, the absorptions due to ether linkage in the parent commercial resin and the parent laboratory-synthesized resin were estimated to be 0.09 and 0.15, respectively. In support of this hypothesis, the heat absorbed at the endotherm (≈ 215°C) was greater in the commercial resin than in the laboratory-synthesized resin (172 cal/g v. 133 cal/g). This may be a reflection on the methylol condensation reaction, indicating that the amount of methylol groups in the commercial resin was greater than that in the laboratory resin.

In general, the first stage of PRF resin synthesis involves the preparation of phenol-formaldehyde (PF) resin from phenol and formaldehyde. At a later stage of the reaction, resorcinol is charged into the reaction vessel. Therefore, the subsequent thermal response of the PRF resin in the presence of additional formaldehyde (in the form of added paraformaldehyde) depends on the
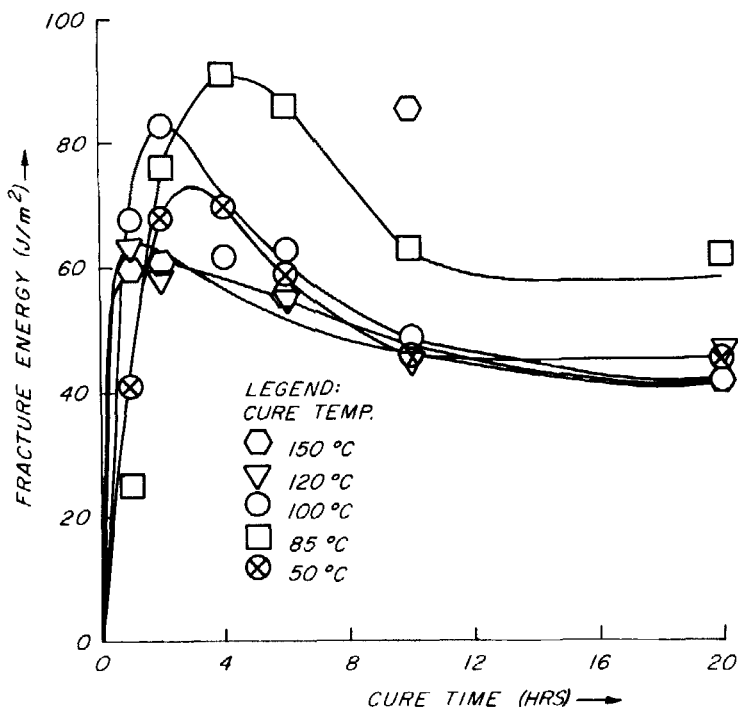
FIGURE 13   Fracture initiation energy as a function of cure time for specimens cured at various temperatures. Note the presence of an optimum for each cure temperature and that, in general, the cure time at which the optimum occurred decreased with increasing cure temperature.

amount and degree of molecular integration of added resorcinol. From the infrared studies, it appears that the ratio of phenol and/or resorcinol to formaldehyde in the parent commercial resin was lower than the same ratio in the parent laboratory-synthesized resin. Consequently, the relative number of available reactive positions on the phenol and/or resorcinol rings may have been considerably greater in the laboratory resin. In this case, the initial methylol groups formed from the added paraformaldehyde immediately condensed further to a dimenthylene ether linkage. Greater amounts of paraformaldehyde resulted in further methylol group formation due to the abundance of reactive positions. However, the ether linkages started to decompose at the same time, possibly due to the highly exothermic nature of methylol substitution. On the other hand, the commercial resin experienced minimal (if any) further methylol group substitution due to the limited available reactive positions (low phenol and/or resorcinol to formaldehyde

ratio). Therefore, the amount of dimethylene ether linkage formed (relative to the pure resin) increased only slightly in correspondence with a slight decrease in the methylol groups. Notice from Figure 4 that the absorption trend of the dimethylene ether linkage is a mirror image of that due to methylol OH group.

Results from GPC and solubility measurements indicate that the observed contrasting infrared absorption characteristics of the laboratory and commercial resins are due largely to the differences in reactivities between the two resins. This difference, in turn, is attributable to the reactive site/formaldehyde ratio which is higher in the laboratory than in the commercial resin. For the parent commercial resin, where the residual reactive positions are low (due to a low resorcinol content and/or high formaldehyde content), the added paraformaldehyde was not incorporated into the molecular structure of the adhesive. Consequently, a considerable portion of the added paraformaldehyde, which was simply occluded in the adhesive, dissolved in the solvent. This accounts for the observed increase in the soluble fraction of the commercial adhesive with increased addition of paraformaldehyde. (It might be necessary to point out that during the grinding of the "cured" commercial resin adhesive, a strong odor of formaldehyde was detected.) On the other hand, for the laboratory resin adhesive, all of the added paraformaldehyde (except possibly at 25 phr added paraformaldehyde) reacted. Consequently, the enhanced degree of crosslinking led to a continuous decrease of the soluble fraction of the adhesive with increased paraformaldehyde concentration.

The reason for the observed trend in fracture energies, with respect to paraformaldehyde addition and the somewhat different trends between the commercial and laboratory-synthesized resin adhesives, is not very clear to us. However, it could be due to a combination of the chemical nature and the physical characteristics of the adhesive in relation to the adherends. As we mentioned in an earlier report,[1] controlled wetting and penetration are two important prerequisites which must be satisfied for the formation of a good joint. For these conditions to be fulfulled, an appropriate viscosity level is imperative. Generally, the attainment of this viscosity level is contingent upon:

    i) the adhesive components
    ii) the assembly time
    iii) the moisture content of wood
    iv) the applied glueline pressure

The last three factors were held as constant as possible in our experiments. Thus, the overriding factor should be the adhesive components.

For the filled commercial resin adhesive, a paraformaldehyde addition of 10 phr was the optimum required to attain the desired toughness level of the adhesive. Beyond this concentration, the resulting initial viscosity may have

been such that controlled wetting and penetration and, hence, proper anchorage of the solid adhesive film was impossible. Consequently, the fracture energy dropped with increased paraformaldehyde addition (see Figure 7). On the other hand, for the unfilled commercial resin adhesive, even at 25 phr added paraformaldehyde either the optimum viscosity was not reached, so that fracture energy increased continuously with increasing paraformaldehyde addition or that with large additions of paraformaldehyde some amount remains unreacted and simply acts as a "plasticizing" filler in the commercial adhesive.

By comparison, for both the filled and unfilled laboratory resin, a higher paraformaldehyde concentration appeared to have been necessary to achieve the optimum viscosity level. This is understandable in light of the fact that the pure commercial resin had an initial viscosity of 665 cp $v.$ 331 cp for the pure laboratory resin. Unlike the case of the commercial resin adhesive, the unfilled laboratory resin adhesive had optimum properties at the same paraformaldehyde concentration as the filled adhesive, $i.e.$, at 15 phr. Recall that from the DSC, IR, GPC, and solubility measurements, the laboratory resin was found to be more reactive than the commercial resin. Solubility measurements, in particular, showed that while the added paraformaldehyde seemed to have been simply occluded into the bulk adhesive (due to lack of reaction) for the commercial resin, in the case of the laboratory resin all the added paraformaldehyde reacted up to 25 phr. Even though the initial adhesive viscosity for the filled and unfilled laboratory adhesives may have been different, the reactivity of the resin is such that, within the assembly period, the optimum viscosity is attained. While the resin solids content determines the optimum viscosity level for the commercial resin (less reactive resin), the solids content and resin reactivity control the achievement of the optimum viscosity for the laboratory resin (reactive resin). It is perhaps not by chance that the optimum fracture energy for the joints from the laboratory resin adhesive corresponds approximately to the paraformaldehyde concentration at which:

a) species III of the soluble fraction of the laboratory resin adhesive decreased to an almost imperceptible level (Figure 5b).

b) drastic reduction in the 1100 cm^{-1} IR band corresponding to disappearance of the dimethylene ether linkage (Figure 3). These chemical changes probably lead to embrittlement of the adhesive.

The higher reactivity of the laboratory-synthesized resin relative to the commercial resin is further reflected by the generally higher fracture energies of joints from this resin adhesive and by the transition from stable to unstable crack propagation in the failure characteristics of mica-filled laboratory resin adhesive-bonded joints.

Thermal effects

The infrared results agree with the contention by Yamao *et al.*[9,10] that the formation of dimethylene ether linkage is a consequence of the condensation of methylol groups. The increase in the absorption band due to ether linkage $(1100\ cm^{-1})$ coincided with the decrease in the absorption due to methylol groups. From the literature, the three possible products of decomposition of the ether linkage, represented by equations 1 to 3, could not be quantitatively discriminated from our infrared results. A discernible decrease in the $2925\ cm^{-1}$ absorption band due to CH_2 stretching vibration (reaction 1) was not observed. A small shoulder at $1650\ cm^{-1}$ due to carbonyl absorption was evident in the infrared spectra (reaction 2). But the trend could not be ascertained because this band was not properly resolved from the $1610\ cm^{-1}$ band (due to benzene ring semi-unsaturation). While some decrease in the phenolic OH group $(1220\ cm^{-1})$ was observed, no bands were observed at $1680\ cm^{-1}$, which would have confirmed the presence of quinone methide type reaction products (reaction 3).

$$(1)$$
$$(2)$$
$$(3)$$
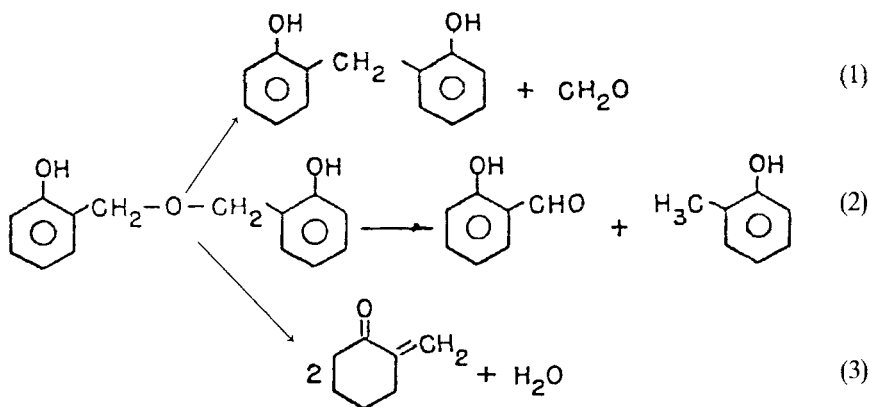
The relative decrease of the soluble fraction of the cured adhesive with increased cure time at cure temperatures of 50, 85 and 100°C are as would be expected. The gel permeation chromatograms show a similar decrease in the amount of species in the soluble fraction. The minima observed for the soluble fractions of the adhesives cured at 120 and 150°C were somewhat surprising. To explain the observed results, we take recourse in the three equations above. It appears that reaction 1 is predominant at low cure temperatures (50 to 100°C) while either reaction 2 or 3, or both, predominate at long cure periods at cure temperatures of 120 and 150°C. The occurrence of chain scission as represented by these reactions may be responsible for the increased amount of soluble products at longer cure times at these temperatures. As we mentioned

earlier, Yamao *et al.*[9,10] had observed the predominance of these reaction paths at high cure temperatures ($T = 120°C$).

The fracture energy shows a strong dependence on cure temperature. Notice that, over the entire cure period, the highest fracture energies were obtained from specimens cured at 85°C. We should point out that DSC measurements showed that 85°C was the temperature at which the exothermic peak maximum (cure temperature) occurred for the adhesive formulation used in these experiments. Thus, it appears that the maximum thermal response of an adhesive occurs at or near the cure temperature of the adhesive giving highest fracture energies. Cure of the adhesive definitely involves a measure of mobility of polymer molecules. At temperatures above and below the optimum cure temperature, polymer chain mobility may be substantially increased or inhibited for proper alignment of the chains for crosslinking. Gillham[14] has observed similar phenomena in other thermosetting resin systems and postulates two temperatures of activity, one associated with the cure temperature and the other associated with the glass transition of a highly crosslinked network.

The fracture energy at each cure temperature also showed a strong dependence on cure time. At each cure temperature, a certain minimum cure time was required for the optimization of joint fracture energy. This cure time minimum generally decreased with cure temperature although specimens bonded at 50°C deviated from this behavior. Notice that the relationship of the fracture energy with cure time at each cure temperature (Figure 13) is almost identical to that of the absorption band assigned to the dimethylene ether linkage (1100 cm^{-1}) (Figure 9). This similarity may not be entirely fortuitous. However, other factors do contribute to joint performance. Pillar,[15] using a free vibrational apparatus, (Dynamic method) studied the rate of strength development with cure. He found that there was little change in strength until the gel transition where a sharp increase occurred. The strength continued to increase during the rubbery state but decreased sharply at the glass transition. He attributed this decrease in strength at the glass transition, or point of onset of rigidity, to internal stresses caused by shrinkage. However, it may be argued that shrinkage is itself a reflection of the chemical changes that have occurred within the adhesive. The degree of crosslinking would be expected to contribute substantially to the shrinkage. But the pattern of behavior of the bands (760 cm^{-1}, Figure 9) suggests little change of the degree of substitution on the benzene ring, and thus no resemblance to the fracture energy trend. The formation and subsequent decomposition of dimethylene ether into the products shown by Eqs. 1 to 3 to provide an explanation to the behavior of fracture energy. For example, chains containing ether linkages are expected to be relatively flexible (stress-relieving). As more of these chains are formed, the fracture energy should increase. However, at the onset of decomposition of

these chains, either into the more rigid methylene bridges or scission products (reactions 2 and 3), a drop in the fracture energy would be predicted.

Implications for durability studies

These series of studies were undertaken within the general context of durability prediction of adhesive joints. Current methods of durability prediction in the wood industry involves subjecting adhesive joints, for short periods, to conditions more severe than they would actually experience under field conditions (i.e., accelerated tests). The rationale for this approach is the desire to reduce the experimental time scale while at the same time inducing, at least in principle, the deterioration that would occur over long periods of time in service. However, no entirely satisfactory correlation between accelerated test data and actual long-term service results have been obtained. Ebewele[16] has pointed out that this discrepancy between accelerated test results and real-time service performance of adhesive joints could be due partly to the arbitrary selection of conditions for accelerated tests. He argued that any two arbitrarily selected time and temperature combinations are not necessarily equivalent. The fracture energy-cure time relationship in Figure 13 provides experimental support for this argument. This figure shows that even at elevated temperatures, long cure times involving several hours is needed to produce stable fracture energies. Hence, accelerated tests at elevated temperatures must take into account this change of property.

Figure 12 indicates that the fracture energy-cure time profiles exhibit a maximum. Thus, for example, points A and B in Figure 12 have the same value of fracture energy. However, the fracture characteristics of adhesive joints with this value of fracture energy are not necessarily the same. Mijovic and Koutsky[17] in a recent paper have made similar observations. They counseled that studies attempting to establish G_{Ic} as a material property should first establish the cure time dependence of G_{Ic}.

A brittleness index, I, which is directly proportional to the difference, $G_{Ic} - G_{Ia}$, is a measure of the resistance of an adhesive system to catastrophic failure. It is obvious from Figure 12 that $I_A \neq I_B$. Besides, as we saw from the results of solubility measurements (Figure 11) the susceptibility to attack from aggressive environments depends on the time and temperature of cure. Thus, two adhesives of the same crack initiation values may behave entirely differently under an aggressive environment. We have previously presented preliminary evidence[1] which showed that for design purposes the G_{Ic} and G_{Ia} profiles divide the fraction energy-cure time envelope into three domains. Load values which yield $G_I > G_{Ic}$ would certainly result in catastrophic failure; those loads which give $G_{Ic} > G_I > G_{Ia}$ may or may not result in failure, depending on environmental conditions; whereas loads which give $G_I < G_{Ia}$

should give stable and durable bonded structures since any cracks, if initiated, should be arrested. The results presented here, therefore, have important practical utility. First, the information furnished about adhesive joint response to various temperature and time conditions can be employed for selecting appropriate bonding conditions for optimal joint performance. Secondly, a more rational approach to durability prediction by the use of equations involving time-timperature superposition is possible.

CONCLUSIONS

The most important conclusion resulting from this work is that fracture behavior, if carefully controlled using fracture mechanics principles in specimen design, can be directly correlated with base resin reactivity and composition, time and temperature of cure, and filler type. Even in the very complicated nature of wood bonding these correlations can be established and be of great utility for adhesive evaluation.

The phenolic resin systems employed, which are typical of many wood glues, indicate that higher resin reactivity due to higher resorcinol content with paraformaldehyde generally indicates:

1) Greater fracture toughness of bonded joints
2) A more durable (less soluble), highly crosslinked resin network
3) Greater interaction with some filler materials.

It is also important to note that the state of cure of the resin can be followed *via* fracture toughness measurements. As cure proceeds, the fracture toughness first increases, maximizes and then decreases to some final value which is constant, independent of cure time. This behavior is quite general and has been observed for a wide variety of resin systems and different adherends. The formation and decomposition of ether linkages with increasing cure time offers an explanation for this behavior in the resins studied here. It should be added that DSC studies are also of great value since maximum fracture toughness was obtained at a cure temperature which coincided with the temperature associated with the resin—paraformaldehyde reaction exotherm on the DSC thermograms.

The optimum paraformaldehyde addition giving maximum fracture toughness is related to the reactivity of the parent resin and generally excessive amounts of paraformaldehyde increases resin solubility and decreases fracture toughness. Unreacted excess paraformaldehyde might act as a "plasticizer" or viscosity modifier which directly relates to fracture toughness and might be important in less reactive base resin systems.

The effects of fillers on fracture toughness is strongly related to the reactivity

of the resin system and is complicated by size and shape effects as well as by filler surface reactivity. This work shows profound effects of filler type on fracture toughness. Mica, a relatively unreactive, weak lamellar filler gave substantially less fracture toughness than walnut shell flour at the same weight fractions. Further studies must be done to clarify the effects of filler on the resin properties such as reactivity and viscosity as well as fracture toughness of the bonded joints.

Finally, the cure temperature and cure time required to produce unchanging fracture toughness and brittleness properties should be established before conducting adhesive durability studies. The use of these conditions to prepare test specimens, especially for elevated temperature, accelerated aging studies, should reduce the test variability and improve the durability prediction of adhesives.

Acknowledgments

References

1. R. O. Ebewele, B. H. River and J. A. Koutsky, *Wood and Fiber* **11,** 197 (1979).
2. R. O. Ebewele, B. H. River and J. A. Koutsky, *Wood and Fiber* **12,** 40–65 (1980).
3. A. Zinke, *J. Appl. Chem.* **1,** 257 (1951).
4. H. von Euler *et al., Ark Kemi Min Geol.* **15A,** No. 11, (1942).
5. K. Hultzch, *Chemie der Phenolharze* (Springer Verlag, Berlin, 1950).
6. H. S. Lilley, *J. Soc. Chem. Ind.* (London) **6,** 196 (1948).
7. R. T. Conley and J. F. Bieron, *J. Appl. Polym. Sci.* **7,** 103 (1963).
8. W. M. Jackson and R. T. Conley, *J. Appl. Polym. Sci.* **8,** 2163 (1964).
9. M. Yamao *et al., Kogyo Kagaku Zasshi* **74,** 2571 (1971).
10. M. Yamao, S. Nukui and S. Tanaka, *Nippon Kagaku Kaishi* **5,** 914–919 (1972).
11. S. Chow, *Holzforschung* **31,** 200 (1977).
12. K. Nakanishi, *Infrared Absorption Spectroscopy* (Holden-Day, Inc., San Francisco, 1962), pp. 26–27.
13. S. Chow and P. R. Steiner, *Holzforschung* **32,** 120 (1978).
14. J. K. Gillham, *AICHE J.* **20,** 1066 (1974).
15. W. O. Pillar, *For. Prod. J.* **16,** 29 (1966).
16. R. O. Ebewele, The Fracture Mechanics Approach to the Assessment of Adhesive Joint Performance in Bonded Wood Products. Ph. D. thesis, University of Wisconsin, Madison, Wis. (1980).
17. J. Mijovic and J. A. Koutsky, *Polymer* **20,** 1095 (1979).